

Fabrication and Optical Behavior of Chiral Thin Film Materials

M.J. Brett, M.O. Jensen, J.C. Sit, S.R. Kennedy, and K.D. Harris, University of Alberta, Edmonton, Canada; and D.J. Broer, Philips Research Laboratories, Eindhoven, The Netherlands

Key Words: Glancing angle deposition (GLAD) Substrate fixture design
Liquid crystal display Morphology

ABSTRACT

The glancing angle deposition (GLAD) technique may be used to fabricate thin films with a very porous chiral or helical microstructure, and with the geometry of the helices controlled to have specific porosity, helical pitch, and handedness. Films with chiral morphology exhibit optical rotation and circular dichroism similar to certain classes of liquid crystals, with the pitch and handedness of the chiral film determining the resultant optical properties. Results will be presented from a study of the optical behavior of chiral films fabricated from materials such as silicon dioxide, alumina, and magnesium fluoride, and from a study of the effects of parameters such as helical pitch, film thickness, and film porosity on the optical properties. The enhancement of optical response created by impregnating these films with nematic liquid crystals (LC) will be reported, and reversible electro-optic switching of the LC component demonstrated. The potential of photonic band gap materials produced by fabricating periodic GLAD films on pre-patterned substrates will be discussed, and the growth of square helices in a tetragonal array presented.

INTRODUCTION

The use of optically active thin layers is desirable in many applications, especially those involving display devices where liquid crystals (LCs) are the conventional tool of choice. Orientation of LC molecules can be controlled by various techniques [1-3]; however, typical methods allow for alignment near the substrate interface only, and do not allow for the possibility of thicker cells. It is then desirable to produce thicker LC cells while still maintaining strong domain ordering of the LC molecules in the goal of producing superior display devices.

In inorganic materials, the first observation of optical activity and circular Bragg reflection in obliquely deposited thin films was with fluorite films by Young and Kowal in 1959 [4]. These films were deposited at conservative oblique angles ($<70^\circ$) and the resulting semi-porous films exhibited rotatory powers up to $155^\circ/\text{mm}$ (amount of rotation per thickness of film). After theoretical work by Lakhtakia and Weiglhofer [5] and Azzam [6], Robbie et al. at the University of Alberta developed the Glancing Angle Deposition (GLAD) technique

for fabrication of highly porous chiral thin films [7-9]. The GLAD process can be used to create porous films with chiral/helical microstructure that is anisotropic with respect to incident circularly polarized light. This circular birefringence is responsible for the optical activity (rotation of linearly polarized light) exhibited by these films. The magnitude of the rotatory power of the film alone is not ideal when compared to denser films deposited at lower angles [10]. However, nematic liquid crystals can be added to the films and a chiral-nematic phase induced in the LC molecules to enhance the optical properties of the hybrid device [11]. This technique would not be possible with more conventional, dense films, and while it improves the overall rotation of the thin film layer, it also allows for dynamic switching [12].

GLAD fabricated chiral thin films also hold a potential for building photonic band gap (PBG) crystals. The principle of PBG crystals is to inhibit the propagation of certain electromagnetic modes in a material with a high, periodic dielectric contrast [13-14]. Manipulation of a PBG material by intentional introduction of defects allows for confinement and guiding of light, with applications in photonics and integrated optics. The inherent porous nature of GLAD thin films immediately provides high dielectric contrasts, and periodicity can be imposed by using pre-patterned substrates. While a chiral microstructure is unsuitable for PBG crystals, other realizable GLAD structures such as square helices are anticipated to yield strong photonic band gaps [15].

FABRICATION AND STRUCTURE OF GLAD THIN FILMS

The GLAD technique for thin film growth uses physical vapor deposition (PVD) at extreme incidence angles, $>80^\circ$ from the substrate normal, to produce highly porous films with porosities of more than 50% [9,16]. Initially, incident flux from the PVD source randomly nucleates on the substrate, and subsequent growth of the thin film evolves exclusively from these nuclei, since the intermediate substrate areas fall in the shadow of the nuclei. Automated control of substrate orientation and rotation with deposition rate feedback from a crystal thickness monitor allows for the creation of films with various porous structures, such as vertical and slanted posts, chevrons/zig-zags [17], helices, and square spirals. The type of structure, as

well as the film porosity, are given by the flux incidence angle (or substrate tilt) α and the substrate rotation φ , as shown in Figure 1a. Substrates with lithographically prepared seed patterns give rise to periodic growth. The macrostructure of a GLAD film can be controlled down to a few tens of nanometers, while the crystallographic microstructure depends on a range of parameters, including film material and deposition temperature.

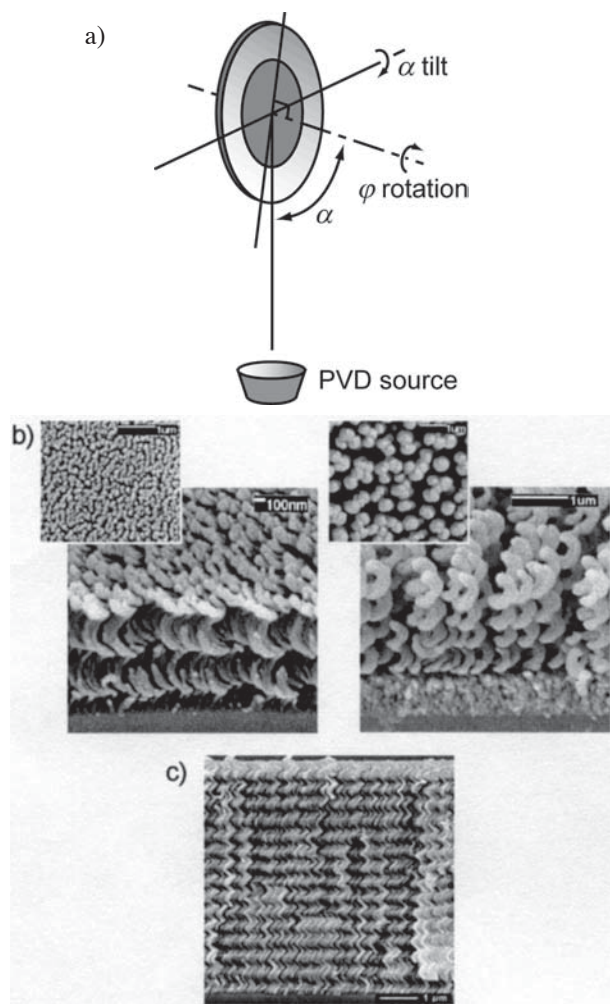


Figure 1: a) Schematic of the GLAD system, showing flux incidence angle α and substrate rotation φ . b) Examples of chiral SiO_2 thin films deposited at $\alpha=83^\circ$ (left) and $\alpha=85^\circ$ (right), with insets showing views from the top. Note the change in porosity with α . c) Example of Si square spiral thin film deposited at $\alpha=85^\circ$.

Optical films use either thermal or electron beam evaporation to deposit dielectric materials such as magnesium fluoride, silica and alumina. In creating GLAD thin films with chiral structure, the substrate is rotated at a constant rate $d\varphi/dt$ relative to the incoming flux rate, while maintaining a fixed incidence angle α . The exact values of the deposition parameters control the chiral structure and specified dimensions, such as helical pitch (defined as the vertical distance between each helical turn), helical radius and handedness. As can be seen in Figure 1b, both the structure and porosity are controlled by the speed of rotation of the substrate and the incidence angle. For square spiral GLAD films the substrate rotation φ is abruptly changed 90° at periodic intervals of accumulated film thickness, with the incidence angle α remaining fixed. Figure 1c shows an example of a GLAD square spiral film.

OPTICAL PROPERTIES OF HYBRID GLAD/LC FILMS

Deposition Incidence Angle and Rotatory Power

At higher incidence angles α the effect of nuclei self-shadowing is greater, and a more porous film is produced. Because it allows for a larger amount of filling by LCs, greater porosity of the films is desirable; however, the disadvantage of creating films at larger angles is that the deposition rate becomes very low due to the cosine dependence of the angle on the amount of flux incident on the substrate. Also, as the film structures become further separated with higher porosities, the ordering of the LC molecules can become more random and the optical effect degraded. Thus, a compromise must be found that balances all of these effects and produces the optimal structure.

Shown in Figure 2 is the rotatory power of GLAD chiral thin films (the polarization rotation per unit thickness of film) as a function of deposition incidence angle α . The first notable trend is the significant increase in rotatory power for hybrid films filled with LCs over their unfilled counterparts, demonstrating the enhancement of the optical properties by the LC molecules [18]. At an incidence angle of 85° , there appears to be an optimum compromise between the aforementioned effects concerning porosities. Thus for chiral GLAD film/liquid crystal hybrid devices, our study is concentrated on films deposited at this angle.

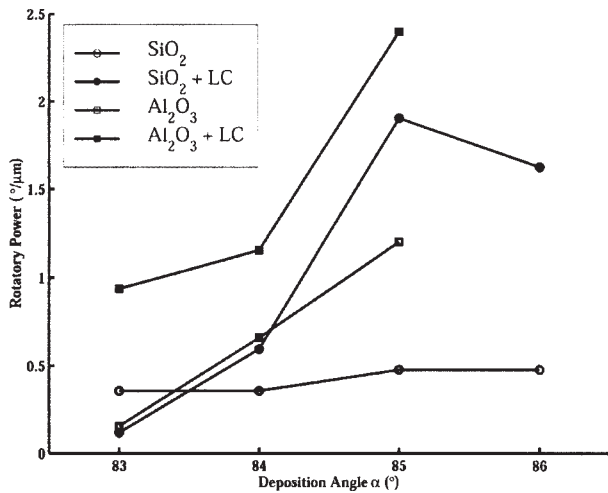


Figure 2: Average effective rotatory power as a function of deposition angle for SiO₂ and Al₂O₃ films, both unfilled and LC filled.

Film Thickness and Rotatory Power

The effectiveness of a film's optical properties is best understood in an investigation of the amount of rotation per unit thickness, or the average effective rotatory power. Figure 3 shows the results of peak rotation values for three film materials of increasing thickness [18]. There is a significant increase in the amount of rotation for the LC filled films; however, the reversal in direction of rotation for MgF₂ and Al₂O₃ films when filled with LCs is unexpected. It is not thoroughly understood from where this phenomenon arises, but it is possible that its roots lie in LC molecule/film structure interactions that are ultimately responsible for the enhancement of the optical properties.

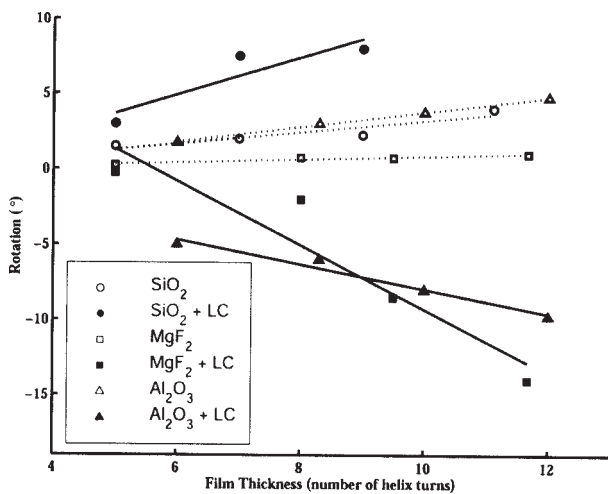


Figure 3: Plots of peak rotation as a function of film thickness for both LC filled and unfilled films of SiO₂, MgF₂ and Al₂O₃. For the MgF₂ and Al₂O₃ films, a reversal in the direction of rotation arises with the addition of LCs.

In Table 1, summarizing the effects of the addition of LCs to GLAD films, it can be seen that a six fold increase in the magnitude of the rotatory power results for the MgF₂ films, and a two fold increase is seen for the rotatory power of the two other film materials. The negative sign for the entries in the right hand column of Table 1 represents the reversal in direction of rotation that was seen in the preceding graphs. The increase in magnitude of the rotatory power for LC filled films is strong evidence that there is a chiral nematic phase induced in the LC molecules by the film structure, and this enhancement can be exploited for these film hybrids.

Table 1: Average effective rotatory power of films and hybrid devices of various optical materials.

Material	Film (°/μm)	Film and LC (°/μm)
MgF ₂	0.16	-0.96
SiO ₂	0.67	1.34
Al ₂ O ₃	1.05	-2.20

In addition to increasing the optical activity of the films, the addition of LCs has two major side-benefits. First, the matrix of the LCs more closely matches the index of refraction of the film materials, and as a result there is less scattering of light in the film/LC hybrids. Secondly, intentionally filling the films reduces the risk of contamination by ambient humidity, which would degrade the effectiveness of the devices [19].

GLAD/LC CELL FABRICATION AND BEHAVIOR

For the fabrication of LC switching cells, chiral thin films of SiO₂ were deposited using GLAD by electron-beam evaporation onto glass substrates coated with indium-tin oxide (ITO) transparent conductor. This film was composed of left-handed helical columns with 8.4 turns and a pitch of 410 nm. The pitch in a helical GLAD film is controlled by the ratio of deposition rate to substrate rotation rate, while the handedness is controlled by the direction of rotation. Liquid crystal switching cells were constructed by using a second ITO-coated glass substrate to form a "sandwich" with the GLAD film in between. The cells were filled with LCs in an evacuated oven by dipping one edge of the cell into a pool of the LC. The cells fill by capillary action and are then sealed. The two glass substrates were offset slightly to permit electrical contact to the ITO layers. We used nematic LC E7 from Merck ($n_o = 1.5216$, $n_e = 1.7462$ at 25°C).

A UV/VIS spectrophotometer was used to perform the measurements. The light path consisted of: light source, depolarizer, linear polarizer, quarter wave retarder oriented at $\pm 45^\circ$ to the polarizer axis, sample, depolarizer, and detector. Left- (LCP) or right-circularly polarized (RCP) light was produced

by the combination of the linear polarizer and the quarter wave plate (560 nm). Transmission was measured for both LCP and RCP, from which difference spectra were calculated.

Figure 4 shows measurements of LCP and RCP transmission from the cell prior to filling with the LC (“unfilled film”), and after filling it, in addressed and unaddressed modes [12]. In the unaddressed state (no voltage applied), enhanced circular dichroism as compared to the unfilled film is observed (“un-addressed” versus “unfilled film”). LCP, the circular polarization which matches the handedness of the film, is selectively scattered/reflected by the sample, as consistent with previous work and theoretical investigations [11, 20]. A remarkable effect was observed when the cell was addressed with a 1 kHz, 200 V (peak-to-peak) signal. In the addressed state, all transmission difference between LCP and RCP vanished. The application of the electric field causes the LC molecules to change their alignment from the quasi-chiral nematic phase to a homeotropic state (perpendicular to the substrates and parallel to the applied electric field). Transmitted light through the cell thus “sees” the ordinary index n_o of the LC (1.52 for E7), which is an approximate index match for the GLAD film material (SiO_2 , $n = 1.47$), causing the chiral nature of the film to be effectively cancelled and resulting in the loss of circular polarization transmission difference. When the electric field was removed, the cell reverted to its unaddressed state.

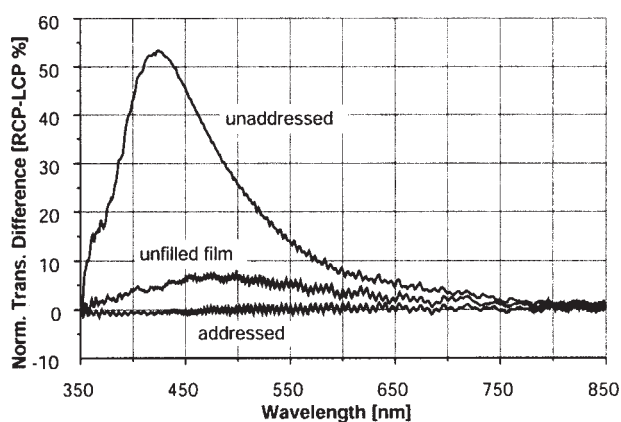


Figure 4: Circular dichroism measurements show the effects of embedding LCs into a GLAD chiral film. The transmission difference RCP-LCP is normalized to RCP transmission. When the cell is addressed, the chiral optic response vanishes.

OPTICAL PROPERTIES OF HELICALLY PERFORATED GLAD FILMS

The preceding sections have dealt with optical properties of chiral films, both unfilled and filled with LCs. It is also possible to fabricate inverse structures such as a thin film with

helical perforations. In this section the fabrication of helically perforated films is described [21], and the optical properties of such films reported. The fabrication proceeded in four steps, using a chiral GLAD film as the initial template for the structure.

Step One - Template Deposition

Chiral GLAD films were fabricated in SiO_2 on glass substrates. Both left and right-handed films were produced.

Step Two – Template Filling

Each of the films was filled with HPR504 photoresist (Arch Chemicals) in a photoresist spinner. The films were spun nominally at 5.5 krpm for 30 s, and subsequently baked in a vacuum environment for 60 s to remove the solvent. The appearance of a film after such processing is shown in Figure 5a. Photoresist has filled the film completely, and no regions devoid of photoresist are apparent.

Step Three – Partial Etchback

It was found necessary to remove a thin layer of photoresist from the top of each filled film in order to enable subsequent etch removal of the template. Each filled film was immersed in Shipley 354 photoresist developer solution for less than 1 s, exposing the tops of the template microstructures. The appearance of one film processed in such a manner is shown in Figure 5b. 550 nm of photoresist have been removed from the top of this film, leaving 900 nm of photoresist remaining to form the perforated film. In this processing step, success in exposing the template microstructure has also been achieved by reactive ion etching of the photoresist in an oxygen plasma.

Step Four – Template Removal

Finally, the perforated film may be completed by immersing the hybrid film in an etch designed to remove the template material. For SiO_2 templates, a 7:1 buffered oxide etch solution (Arch Chemicals) containing F-ions was utilized. Figure 5c shows a scanning electron microscope (SEM) image of a perforated film. Helically perforated films have also been produced in spin-on-glass.

Optical rotation measurements were made on four films fabricated by the methods above: an SiO_2 right handed chiral film of 2800 nm thickness consisting of 12 turns; a perforated film of this structure in HPR504 photoresist; an SiO_2 left-handed film of 3800 nm thickness consisting of 12 turns; and a perforated film of this structure in HPR504 photoresist. Measurements were also made on an uncoated glass slide and a photoresist coated glass slide, as references for the experiment. Table 2 shows the experimental results, giving the average rotation between 400 and 650 nm in each case.

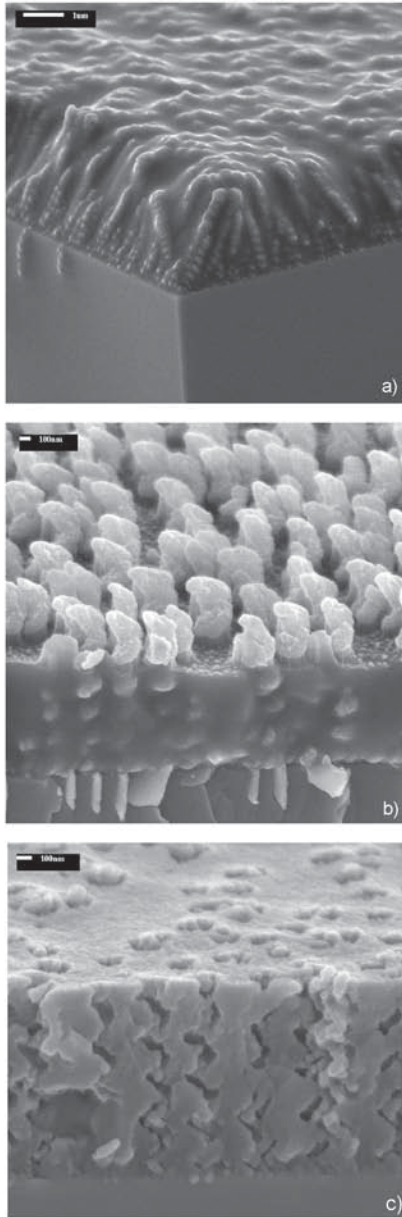


Figure 5: Images showing steps in the fabrication of helically perforated films. Note that the images are not from the same template film. a) Chiral film filled with photoresist to the top of the helices, with no voids evident. b) A thin layer of photoresist has been removed from the top of the film in preparation for further processing. c) A helically perforated thin film of photoresist.

Table 2: Polarization rotation by chiral and perforated GLAD thin films.

Test Sample	Rotation ($^{\circ}$)
Glass slide	-0.03
Glass slide, photoresist coated	-0.07
Left-handed template film	+0.49
Left-handed perforated film	-1.48
Right-handed template film	-1.53
Right-handed perforated film	+3.93

The results show expected rotations for the left and right-handed template (chiral) films, although the right-handed film gave a stronger rotation for reasons not clear at this time. The perforated films show a reversal of rotation from their respective templates, since the refractive index gradient has been inverted with an air helix ($n=1$) surrounded by a photoresist matrix ($n\sim 1.6$). The stronger optical activity of the perforated films (a factor of three) bears further study, as the refractive index of the photoresist is not significantly different from that of SiO_2 .

FABRICATION OF PHOTONIC BAND GAP STRUCTURES USING GLAD

The basis of a photonic band gap (PBG) material is a periodic structure with a high dielectric contrast, where complex scattering of electromagnetic waves leads to gaps in the ordinarily continuous bands of allowed propagation modes. Furthermore, in order to achieve PBG effects for the application rich regions of visible and infrared light, the length scale of the periodicity of the PBG structure must be of the same order of magnitude as the wavelength of the light, i.e. as low as a few hundreds of nanometers. These requirements are quite easily met in one and two dimensions (e.g., in Bragg gratings and lithographically patterned thin films) [22], but fabrication of three-dimensional PBG structures for visible light wavelengths has proven to be a major experimental challenge.

GLAD thin films succeed in addressing the requirements for fabricating PBG structures. First, the high porosity combined with the ability to deposit dielectric materials with high refractive indices (such as Si, SiO_2 and MgF_2) provides large

dielectric contrasts. Secondly, using substrates with periodic patterns of nucleation seeds forces the GLAD film growth to be periodic in the plane parallel to the substrate, while the regular turns of the interwoven GLAD helices provide structural periodicity in the third and critical dimension perpendicular to the substrate. The deposition parameters α and φ together with the layout of the substrate seed pattern, in particular the seed lattice spacing, determine the three dimensional periodicity of the GLAD film, and thus eventually its PBG characteristics. Numerous variations are possible, including the aforementioned square spirals (four-sided helices on a tetragonal seed lattice), hexagonal spirals (six-sided helices on a trigonal or honeycomb seed lattice), and triangular spirals (three-sided helices on a trigonal lattice).

The square spiral approach is the most promising for fabricating GLAD PBG crystals. In this case the film resembles a diamond lattice, and calculations performed by Toader and John show that a square spiral GLAD film will have a large band gap of 15% of the gap centre frequency [15]. The perforation technique described above makes it possible to invert the PBG structure, which can lead to increased band gaps. For the square spiral GLAD film, inversion gives a calculated band gap of 24% of the gap centre frequency.

Figure 6 shows a Si square spiral film on a tetragonal lattice, fabricated using GLAD. The patterned substrate for the film was prepared using traditional photolithography, and featured seeds with a width of 500 nm and a spacing of 1 μm [23]. This and similar uniform GLAD PBG films are intended to show the presence of a basic band gap. In order to be useful for guidance and manipulation of light, however, point and line defects must be introduced along which light can be confined and propagate. This can be achieved by using electron beam lithography, and selectively leaving out individual seeds or rows of seeds during writing of the seed pattern on the substrate [24]. Earlier experiments indicate that GLAD films grow robustly on substrates with defects; The defects do transfer to the film (the extreme flux incidence angle ensures that there is no flux coverage of the seedless defect area), while uniformity of the film is preserved outside of the defects [25].

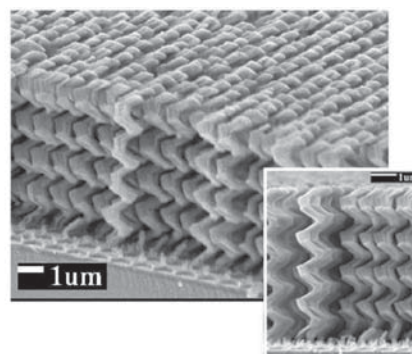


Figure 6: SEM images of GLAD fabricated silicon square spiral film. The tetragonal substrate seed pattern has a seed width of 500 nm and a lattice constant of 1 μm .

CONCLUSION

The addition of nematic LCs to porous GLAD thin films has been shown to improve the optical activity of the films. Chiral films embedded with LCs exhibit enhanced rotatory power and transmission difference between right- and left-circularly polarized light as compared to an unfilled chiral film. These results suggest that the enhancement of the activity is due primarily to the chiral backbone that the film structure provides for the LC. However, it was observed that MgF_2 and Al_2O_3 films had a reversal of rotation upon filling, a phenomena that is not understood and is currently under further study. Inverse structures, or helically perforated films, have been found to exhibit a reversal in optical rotation due to the change in relative refractive indices of the helix and matrix portions of the film. We have also demonstrated electro-optic switching of the LC component in LC filled chiral films when it is addressed within a switching cell. Periodic GLAD films satisfy the fabrication requirements for three-dimensional PBG crystals. We have shown the growth of square spirals on tetragonal seed arrays, which are expected to have a large band gap. Further studies into the optical and structural behavior of GLAD PBG films are currently in progress.

The authors gratefully acknowledge financial support from the University of Alberta, Philips Research Laboratories, the Natural Sciences and Engineering Research Council of Canada (NSERC), Micralyne Inc., and the Alberta Informatics Circle of Research Excellence (iCORE). We would also like to thank George D. Braybrook for providing SEM analyses.

REFERENCES

1. V.H. Zocher, *Naturwissenschaften*, 13, 1015, 1925.
2. J.L. Janning, "Thin film surface orientations for liquid crystals," *Appl. Phys. Lett.*, 21, 173, 1972.
3. W. M. Gibbons, P. J. Shannon, S.T. Sun and B.J. Swetlin, "Surface-mediated alignment of nematic liquid crystals with polarized laser light," *Nature*, 351, 49, 1991.
4. N.O. Young and J. Kowal, "Optically active fluorite films," *Nature*, 183, 104, 1959.
5. A. Lakhtakia and W.S. Weiglhofer, "On light propagation in helicoidal bianisotropic mediums," *Proc. R. Soc. Lond.*, A448, 419, 1995.
6. R. Azzam, "Chiral thin solid films: Method of deposition and applications," *Appl. Phys. Lett.*, 61, 3118, 1992.
7. K. Robbie, M. J. Brett, and A. Lakhtakia, "First thin-film realization of a helicoidal bianisotropic medium," *J. Vac. Sci. Technol.*, A13, 2991, 1995.
8. K. Robbie, M. J. Brett, and A. Lakhtakia, "Chiral Sculptured thin films," *Nature*, 384, 616, 1996.
9. K. Robbie and M. J. Brett, "Sculptured thin films and GLAD (Glancing Angle Deposition): growth mechanics and applications," *J. Vac. Sci. Technol.*, A15(3), 1460 (1997).
10. I. Hodgkinson, Q. Wu, A. Lakhtakia, and K. Robbie, "Vacuum deposition of chiral sculptured thin films with high optical activity," *Appl Optics*, 39, 642, 2000.
11. K. Robbie, D.J. Broer, and M.J. Brett, "Chiral nematic order in liquid crystals imposed by an engineered inorganic nanostructure," *Nature*, 399, 764, 1999.
12. J.C. Sit, D.J. Broer, and M.J. Brett, "Alignment and switching of nematic liquid crystals embedded in porous chiral thin films," *Liquid Crystals*, 27, 387, 2000.
13. S. John, "Strong Localization of Photons in Certain Disordered Dielectric Superlattices," *Phys. Rev. Lett.*, 58, 2486, 1987.
14. E. Yablonovitch, "Inhibited spontaneous emission in solid-state physics and electronics," *Phys. Rev. Lett.*, 58, 2059, 1987.
15. O. Toader and S. John, "Proposed Square Spiral Microfabrication Architecture for Large Three-Dimensional Photonic Band Gap Crystals," *Science*, 292, 1133, 2001.
16. K. Robbie and M. J. Brett, U.S. Pat. #5,866,204, "Method of Depositing Shadow Sculpted Thin Films," 1999.
17. K. Robbie, C. Shafai, and M.J. Brett, "Thin films with nanometer scale pillar microstructure," *J. Materials Research*, 14, 3158, 1999.
18. S.R. Kennedy, J.C. Sit, D.J. Broer, and M.J. Brett, "Optical activity of chiral thin film and liquid crystal hybrids," *Liquid Crystals*, 28, 1799, 2001.
19. I.J. Hodgkinson, Q.J. Wu, and K.M. McGrath, "Moisture adsorption effects in biaxial and chiral optical thin film coatings," *Engineered Nanostructural Films and Material (Proc. SPIE)*, 3790, 184, 1999.
20. A. Lakhtakia and W.S. Weiglhofer, "On light propagation in helicoidal bianisotropic mediums," *Proc. Royal Soc. London*, A448, 419, 1995.
21. K.D. Harris, K.L. Westra, and M.J. Brett, "Fabrication of Perforated Thin Films with Helical and Chevron Pore Shapes," *Electrochem. Solid State Lett.*, 4(6), C39, 2001.
22. A. Polman and P. Wiltzius, "Materials Science Aspects of Photonic Crystals," *MRS Bulletin*, 608, August 2001.
23. S. Kennedy, M.J. Brett, O. Toader, S. John, "Fabrication of Tetragonal Square Spiral Photonic Crystals," *Nanoletters*, 2(1), 59, 2001.
24. M.O. Jensen, S.K. Kennedy, M.J. Brett, "Fabrication of Periodic Arrays of Nanoscale Square Helices," *Functional Nanostructured Materials through Multiscale Assembly and Novel Patterning Techniques (Proc. MRS)*, In Press, 2002.
25. M. Malac, R.F. Egerton, M.J. Brett and B. Dick, "Fabrication of Submicrometer Regular Arrays of Pillars and Helices," *J. Vac. Sci. Technol. B*, 17(6), 2671, 1999.